RSC Advances

This is an *Accepted Manuscript*, which has been through the Royal Society of Chemistry peer review process and has been accepted for publication.

Accepted Manuscripts are published online shortly after acceptance, before technical editing, formatting and proof reading. Using this free service, authors can make their results available to the community, in citable form, before we publish the edited article. This *Accepted Manuscript* will be replaced by the edited, formatted and paginated article as soon as this is available.

You can find more information about *Accepted Manuscripts* in the Information for Authors.

Please note that technical editing may introduce minor changes to the text and/or graphics, which may alter content. The journal's standard Terms & Conditions and the Ethical guidelines still apply. In no event shall the Royal Society of Chemistry be held responsible for any errors or omissions in this *Accepted Manuscript* or any consequences arising from the use of any information it contains.

ROYAL SOCIETY OF CHEMISTRY

www.rsc.org/advances

Ti-O based nanomaterials ameliorate experimental autoimmune encephalomyelitis and collagen-induced arthritis

T. Sree Latha[1], Dakshayani Lomada[1], Praveen Kumar Dharani[2], Shankar V Muthukonda [2] and Madhava C. Reddy[3*]

[1]*Department of Genetics and Genomics, Yogi Vemana University, Kadapa, AP 516 003, India.*

[2]*Nanocatalysis and Solar Fuels Research Laboratory, Department of Materials Science and Nanotechnology, Yogi Vemana University, Kadapa, AP 516 003, India.*

[3]*Department of Biotechnology and Bioinformatics, Yogi Vemana University, Kadapa, AP 516 003, India.*

---

* Corresponding author. Tel.:+91-9703599690; Fax: +91-8562225419

E-mail address: cmreddy@yogivemanauniversity.ac.in or cmadhavareddy@gmail.com.

RSC Advances Accepted Manuscript

Abstract

Multiple Sclerosis (MS) and rheumatoid arthritis (RA) are the most common chronic autoimmune inflammatory diseases that affect central nervous system and joints respectively. Treatment of autoimmune diseases usually concentrates on alleviating symptoms. High-mobility group box 1 protein (HMGB1) cytokine had been reported to play a key role in autoimmune disorders as HMGB1 levels correlate with active inflammation and neutralizing HMGB1can rescue from various autoimmune diseases. Nano-size titania (TiO_2) is an exceptional multi-functional material that showed several practical applications ranging from pigments in paints, UV light absorbent in sunscreen lotion to coatings on non-fogging surfaces, biomedicine and agriculture. However, the *in vivo* role of Ti-O based nanomaterials in autoimmune disease models has not been examined. This study was designed to investigate the role of Ti-O based nanomaterials such as $H_2Ti_3O_7$ nanotubes (TNT) and anatase TiO_2 fine particles (TFP) in well established animal models experimental autoimmune encephalomyelitis (EAE) and collagen induced arthritis (CIA). We showed for the first time that the administration of Ti-O based nanomaterials attenuated clinical signs of pathophysiology and correlated with the reduction of the pro-inflammatory cytokine HMGB1. The clinical signs, histology and HMGB1 secretion data showed that the therapeutic role of TNT and TFP in EAE and TNT in CIA. Thus, TNT and TFP have potential applications in specific treatment of MS/RA and it may provide an effective novel therapeutic approach for other autoimmune diseases.

Keywords

Collagen induced arthritis, Experimental autoimmune encephalomyelitis, HMGB1, TiO_2 nano fine particles, Titania.

RSC Advances Accepted Manuscript

Introduction

Autoimmune diseases are caused by a failure of peripheral T-cell tolerance, resulting in the imbalance of immunoregulatory and inflammatory processes. Most common diseases attributed to autoimmune disorders are multiple sclerosis (MS), rheumatoid arthritis (RA), systemic lupus erythematosis (SLE), myasthenia gravis, pernicious anemia, and scleroderma. MS is an immune-mediated, demyelinating and neurodegenerative disease affecting central nervous system (CNS) [1]. MS approximately affecting 2.5 million people are preferentially young adult women worldwide [2]. The widely accepted animal model of MS is experimental autoimmune encephalomyelitis (EAE) to study the pathophysiology of the disease induced in rodents using self-antigenic epitope peptides from myelin oligodendrocyte glycoprotein (MOG), myelin basic protein (MBP) and proteolipid protein (PLP)[3]. In the current study MOG_{35-55} peptide is used, which is a powerful antigen inducing EAE in C57BL/6 mice[4]. Subsequently Spargue-Dawley (SD) rats were used to induce arthritis by collagen-induced arthritis (CIA) model which shares many clinical, pathological and immunological similarities with rheumatoid arthritis (RA) in human [5]. RA is a systemic, chronic autoimmune inflammatory disease characterized by synovial hyperplasia that affects the joints and other tissues in the body [6]. Though the exact causes of RA and MS are not known, but role of various inflammatory immune cells and network of cytokines were evidenced to be involved in disease progression [7]. High-mobility group box 1 protein (HMGB1) is a ubiquitous DNA-binding protein, released from activated immune cells or damaged, dying cells during necrosis and during the late phase of cellular apoptosis [reviewed in refs.8,9]. Extracellular HMGB1 binds to receptors such as RAGE (receptor for advanced glycation end-products), Toll-like receptor (TLR)-2, TLR-4 and intracellular receptor TLR-9 [10, 11] and results in production of a spectrum of pro-inflammatory cytokines, such as IL-1β, TNF-α, IL-6, IL-8 [12] and chemokines [13]. It has been reported that HMGB1 plays a key role in autoimmune disorders including multiple sclerosis (MS) [14] and rheumatoid arthritis (RA) by mediating the proliferation of T cells in response to anti-CD3 antibody and RAGE[15]. Reynolds *et al.* found that TLR4 expression by T cells is essential for the development of EAE and TLR4 $^{-/-}$ animals efficiently abrogated the EAE disease symptoms. Further, it has been suggested that TLR4 dependent pathways are very essential for induction of EAE, which were involved in development and recruitment of leucocytes in the autoimmune CNS disease[16]. Furthermore, VGX-1027 [(S,R)-3-phenyl-4,5-dihydro-5-isoxasole acetic acid] acts as antagonist for TLR4 and

RSC Advances Accepted Manuscript

significantly slower progression of the arthritic disease with lower clinical and histological arthritic score by inhibiting the cytokines such as IL-1β, TNF-α and IL-10, which play an important immunopharmacological role[17]. In Active lesions of MS/EAE and synovium of RA/CIA, HMGB1 levels correlate with active inflammation [18, 19]and neutralizing HMGB1 antibody can rescue mice from EAE [20, 21] as well as rats from CIA[22]. Malhotra and co-workers found that MS patients showed increased mRNA and protein levels of HMGB1, particularly in patients with relapsing-remitting MS and secondary progressive MS as compared to healthy controls[23]. These facts suggest that HMGB1 plays a critical role in MS/EAE and RA/CIA and it is the target for therapeutic treatment of autoimmune disorders.

Non-steroidal anti-inflammatory drugs (NSAIDs), glucocorticoids and immunosuppressants are usually used as autoimmune disease treatment[24]. However, these drugs have side effects and their toxicity leads to other diseases. Recently use of nanomedicines increased enormously and nanomaterials were shown to offer promising strategies to optimize and improve the treatment of autoimmune disorder. Moreover nanomedicine based therapy has the ability to overcome the limitations of current immunosuppressive and biological therapies[25 26, 27]. The restoration of immune tolerance and using nanoparticles (NPs) is a crucial for autoimmune therapy. More recently, Maldonado *et al*. showed that, pegylated PLGA rapamycin and $OVA_{323-334}$ NPs significantly reduced the production of OVA-specific IgG[28]. Yeste *et al*. using the MOG_{35-55} or PLP_{39-151} EAE model, pegylated gold NPs loaded with the aryl hydrocarbon receptor 2-(1'H-indole-3'-carbonyl)-thiazole-4-carboxylic acid methyl ester (ITE) and MOG_{35-55} or PLP_{39-151} were tested for their ability to ameliorate disease, these NPs successfully suppress the EAE [29]. Dexamethasone (Dex) has been used for evaluating the effects of both prophylactic and therapeutic treatments in different forms of rodent EAE[30]. Dexamethasone ameliorate the development of EAE by increased frequency of autoantigen-specific IFNγ secreting lymph node mononuclear cells. Administration of dexamethasone to the CIA in rodents, suppress the foot swelling and decrease of bone mineral density by inhibiting the overproduction of inflammatory cytokines[31, 32]. Cyclophosphamide has been reported to treat not only cancer, but also autoimmune diseases. However cyclophosphamide was unable to influence the clinical course of EAE in either MOG induced EAE in C57Bl/6 mice or PLP- induce EAE in SJL mice suggesting that these models may be refractory to immunopharmacological manipulation by

RSC Advances Accepted Manuscript

cyclophosphamide [33]. Nanoscience and technology has been witnessing an exponential growth in research and development on material synthesis, properties and its applications. Nanomaterials composed of particle size ≤ 100 nm are exciting due to their extraordinary physico-chemical properties such as high specific surface area and surface-to-volume ratio resulting unique properties than that of their bulk counterpart. Often these materials showed enhanced biocompatibility of biological cells. Previous studies have reported that fullerene nanoparticles and it derivatives accumulate in the joints of murine and effectively inhibit the inflammatory cascade in CIA[34 35 36]. Furthermore, suppression of CIA in rats without toxic effects on the internal organs by intra-articular administration of 13-nm gold nanoparticles (AuNPs) with a concentration of 180-μg/mL[37 38]. Nagai *et al*. stated that, adjuvant induced arthritis (AA) in rats can be treated with gel ointment containing tranilast nanoparticles[39]. A biodegradable polymer poly (lactic-co-glycolic acid) (PLGA) nanoparticles entrapping type II collagen (CII) when administration of administered 3mg PLGA- containing 40μg CII, result in the significantly lower mean arthritis score and severity CIA in mice[40].

Titania is widely used in a number of industrial applications ranging from pigments in paints, UV light absorbent in sunscreen lotion to coatings on non-fogging surfaces. It has been recognized that properties of nano structured titania are different from the bulk form, which could lead to new applications or provide better materials for existing ones. Nano-sized titania based materials have showed excellent photo catalytic properties, anticorrosion, high stability and good biocompatibility [41, 42]. Titanium and its alloys are widely used as orthopedic implant materials includes hip and dental implants[43, 44] as well as jaw fractures[45]. The combination of doxorubicin- TiO_2 effectively enhancing the anticancer efficacy in human SMMC-7721 hepatocarcinoma cells[46]. An improvement in cancer cells killing was demonstrated using photocatalytic action of antibody-TiO_2 biconjugates[47]. Schanen *et al*. reported the immunomodulatory properties of TiO_2 in human peripheral blood mononuclear cells[48]. However, the toxic effect of nano- TiO_2 remains debatable, as conflicting reports have showed that, after initial absorption of nano- TiO_2 can be distributed to other organs and tissues in the body. Thus, nano- TiO_2 interact with plasma membrane exerts genotoxicity via reactive oxygen species induction[49]. Xu J *et al*. demonstrated that intragastric and intravenous injection of TiO_2 nanoparticles at high doses in mice, because acute toxicity effects in the brain, lung, spleen, liver

RSC Advances Accepted Manuscript

and kidney[50]. Recent studies reported that TiO_2 NPs are more toxic than TiO_2 fine particles (FPs)[51]. Oberdorster et al. demonstrated that TiO_2 NPs caused a greater pulmonary inflammatory response than TiO_2 FPs at same mass burden [52]. Although the roles of TiO_2 nanomaterials have been shown in several biological applications, no literature exists on the role of these materials in autoimmune disease.

Here we report for the first-time, $H_2Ti_3O_7$ nanotubes have therapeutic role in well established autoimmune disease animal models EAE and CIA. The results are compared with commercially available anatase TiO_2 fine particles as standard material to repeat the experiments in future and to explain the morphology effect. The clinical signs, histology and HMGB1 secretion data show that therapeutic role of TNT and TFP in EAE and TNT in CIA.

Materials and Methods

Materials

RPMI-1640, Dulbecco's modified Eagles Medium (DMEM), phosphate buffered saline (PBS), antibiotic solution (ABS) and fetal bovine serum (FBS) were purchased from Invitrogen. Lipopolysaccharide (LPS), 3-(4, 5-dimethylthiazol-2yl)-2, 5-diphenyl tetrazolium bromide (MTT), tryphan blue and mitomycin C were purchased from Sigma; Dulbecco's phosphate buffered saline (DPBS), 0.05% Typsin-EDTA and EZcount^{TM} MTT Cell Assay Kit from Himedia Laboratories, India; MOG_{35-55} peptide, complete Freund's adjuvant (CFA), pertusis toxin from Hooke laboratories Inc, MA, USA; bovine type II collagen and HMGB1 Detection Kit from Chondrex Inc., WA, USA.

Synthesis of $H_2Ti_3O_7$ nanotubes

The protonic trititanate ($H_2Ti_3O_7$) nanotubes were synthesized by alkaline hydrothermal method as reported earlier[53]. In a typical synthesis, TiO_2 fine particles denoted as TFP (TiO_2 LAB, Merck, India) dispersed into 10 M NaOH aqueous solution was transferred in Teflon-lined stainless steel autoclave and heated at 130°C for 20 h. The white precipitate was washed twice with distilled H_2O, dil. HCl and C_2H_5OH, finally dried at 80°C for 12 h, the bright white powder denoted as TNT. Endotoxin content analysis of the NPs was performed using Limulus

RSC Advances Accepted Manuscript

amebocyte assay to determine the level of endotoxin in the TiO_2 nanomaterials. The amount of endotoxin detected in 1µg of the TFP and TNT injected into mice was 0.4 and 0.35pg respectively, which did not stimulate production of any cytokines in the mouse ligated ileal loops.

Characterization Techniques

Powder X-ray diffraction (PXRD) data were recorded using a D8 ADVANCE X-ray diffractometer (Bruker), with $\lambda_{CuK\alpha}$ =1.54056 Å. Transmission electron microscopy (TEM) measurements were carried out by using a FEI Tecnai F20ST electron microscope operated at 200 keV, equipped with high angle annular dark field (HAADF) detector and energy dispersive X-ray (EDX) spectrometer. For the TEM measurements, all samples were sonicated in ethanol and the resulting dispersions were transferred on to holey carbon coated copper grids (200 mesh). The particle size and surface charge (zeta potential) of TFP and TNT was measured by using zeta analyzer (SZ-100- Horiba, Japan) to find out the possibilities of any charge based interaction.

Cell culture and HMGB1 quantification

The murine macrophage RAW264.7 cell line was obtained from National Centre for Cell Science (NCCS), Pune, India and cultured in DMEM medium supplemented with 10% FBS, 1% penicillin- streptomycin incubated at 37°C in 5% CO_2 incubator. Cells were plated at a density of $1x10^6$ cells/ well in a 6 well plate and treated with LPS in the presence or absence of TNT or TFP at a concentration of 50µg/ml for 24h. The supernatants were collected and stored at -80ºC until use. The level of HMGB1 in supernatants was detected using HMGB1 ELISA detection kit (Chondrex Inc., WA, USA) according to the manufacturer's instructions.

Animals

Female C57BL/6 mice at 8-10 weeks of age (20-22 g) and female Spargue-Dawley (SD) rats at 6-8 weeks of age (180-200 g) were housed in free of murine specific pathogens under optimal conditions of hygiene, temperature, humidity, light (cycles of 12h dark/light) and fed with standard rodent chow and water *ad libitum*. Experimental animal protocols were approved by the Institutional Animal Ethics Committee (IAEC) and all procedures were conducted in accordance with the “Guide for the Care and Use of Laboratory”.

RSC Advances Accepted Manuscript

Toxicity Studies

Mixed lymphocyte reaction (MLR) was used to measure *in vitro* toxicity of nanomaterials by measuring the proliferation of splenocytes. MLR was carried out as previously described, with some modifications [54]. Splenocytes were isolated from 6-8 week-old C57BL/6 (H-2^b) mice and incubated ($1x10^6$cells/ml) with different concentrations of TNT and TFP for 24 h at 37° C in a humidified 5% CO_2 incubator. Cells were inactivated with mitomycin C for 30 min, washed and used as stimulators. Splenocytes of BALB/c (H-2^d) mice were used as responders. Stimulators (0.01×10^6 cells/ml) and responders (0.1×10^6 cells/ml) were co-cultured in a flat bottom 96 well plate for three days. Proliferation response was measured by MTT assay using EZcount™ MTT Cell Assay Kit (Himedia Laboratories, India) according to the manufacturer's instructions.

EAE induction, treatment and assessment

Mice were randomly divided into four groups (n=5), namely control, EAE, EAE-TNT and EAE-TFP. Mice were immunized for EAE induction with Hooke kits (Hooke laboratories Inc, MA, USA) according to the manufacturer's instructions. Briefly, a volume of 0.1ml emulsion of MOG_{35-55} peptide in complete Freund's adjuvant was injected on either side of the back subcutaneously for each mouse (0.2 ml/animal). Additionally, at days 0 and 1, mice were administered 200ng pertusis toxin *via* intraperitonially. Among them, EAE-TNT group received 15mg/kg (in PBS) of TNT and to EAE-TFP group TFP through intraperitonially on days 7 and 14 from the day of EAE induction. Clinical signs of EAE were assessed according to following score: 0, no signs of disease; 1, loss of tone in the tail; 2, hind limb weakness or partial paralysis; 3, complete hind limb paralysis; 4, front and hind limb paralysis; 5, moribund state.

Arthritis induction, treatment and assessment

Rats were randomly divided into three groups (n=5), namely control, CIA and CIA-TNT. The animals were anesthetized with ketamine and then injected intradermally with 100µl of the bovine type II collagen (2mg/ml in 0.05M acetic acid) emulsified in Freund's complete adjuvant and Freund's incomplete adjuvant on days 0 and 7, respectively at the base of the tail. Subsequently, on the day of immunization rats were given subcutaneously 100µl of PBS alone or with TNT (15mg/kg body weight) at the base of the tail. The levels of arthritis were evaluated according to the arthritis score every two days by two independent observer's up to the day of

RSC Advances Accepted Manuscript

sacrifice (21day). Score condition; 0=normal, 1= mild swelling and redness, 2= moderate redness and swelling of ankle of wrist, 3=severe redness and swelling of the entire paw including digits, 4= maximally inflamed limb with involvement of multiple joints.

Histology

For histological analysis brain and spinal cord were fixed in 10% neutral buffered formalin, dehydrated in 70% ethanol and processed for paraffin embedding. 4µm sections were cut on a microtome and placed on a glass slides, deparaffinised and stained with hematoxylin/eosin (H & E) and Luxol fast blue to evaluate inflammatory infiltrates and degree of demyelination.

For histopathology assessment, paws and knees were removed and fixed in 10% buffered formalin. Sections of paraffin-embedded ankle joints were prepared, stained with H & E and histophathological scoring was done based on density of resident stromal cells and inflammatory infiltrates. Score 0-1 was graded as normal or no synovitis, score of 2-4 as low grade synovitis and score 5-9 as high grade synovitis [55].

T cell Proliferation assay

The effect of TNT and TFP on neural MOG_{35-55} antigen -induced T cell proliferation was measured by MTT assay. To determine the *ex vivo* response, the mouse spleen cells were isolated on day 23 of EAE, EAE-TNT, EAE-TFP mice and cultured in RPMI medium supplemented with 10%FBS in 96-well plate ($2x10^5$ /200µl/well) with 20µg/ml MOG_{35-55} peptide. After 24h, 48h and 72h incubation MTT assay was performed.

Detection of HBGB1 levels

Mice of EAE and rats of CIA were sacrificed at onset or peak of disease and blood was collected into a fresh tube by cardiac puncture. Blood samples were centrifuged for 15 min at 5000g, and serum was transferred to new tubes and stored at -80° until use.

Splenocytes ($2x10^6$cells/well) were prepared from different groups of mice and plated in 24well plate. Cells were re-stimulated with MOG_{35-55} peptide (20µg/ml), culture supernatants were collected after 48h and stored at -80^0C until use. HMGB1cytokine concentration in serum and culture supernatants was measured using HMGB1 Detection Kit (Chondrex Inc., WA, USA) according to the manufacturer's instructions.

RSC Advances Accepted Manuscript

Statistical analysis

Each experiment was repeated three times with n = 5 animals per group. Values were expressed as means ± SD. Data were analyzed with the unpaired t tests and two-way analysis of variance (ANOVA), using Prism 5 software (GraphPad Software, CA). Statistical significance was defined as $P < 0.05$.

Results

Characterization of Titania based materials

Transmission Electron Microscopy (TEM) was used to characterize the titania based materials such as TiO_2 fine particles (TFP) and titanate nanotubes (TNT) and images are displayed in Fig.1. The TFP image shows flakes-like fine particles with high agglomeration. The particle size ranges from 60 - 160 nm, random dark spots in the images are due to alignment of particles one on the other (Fig. 1A). The TEM images of TNT shows nanotubular morphology having 3-5 layers of wrapped nanosheets , having cylindrical in shape with hollow inside and open at both ends. The inner diameter of tube is 3 to 4 nm and outer diameter having various sizes is 8 to10 nm and length is between 100 to 300 nm as shown in Fig. 1B and C.

The X-ray diffraction pattern of TFP exhibited characteristic peak at $2\theta = 25.4^0$ confirms the tetragonal structure with anatase phase (JCPDS NO. 21-1272) as shown in Fig. 2A. The characteristic diffraction peak of TNT exhibited at $2\theta = 10.2^0$ indicates the presence of typical layered crystal structure (Fig. 2B). All other peaks centred at $2\theta = 24.1$, 28.3, and 48.2^0 can be well indexed as the monoclinic structure of $H_2Ti_3O_7$ (JCPDS No.47-0561). During hydrothermal synthesis, anatase phase of TFP particles undergoes dissolution in alkaline solution and crystallized the new material having layered $H_2Ti_3O_7$ phase with monoclinic structure. The BET surface area analysis of TFP and TNT showed interesting results such as 5.1 and 286 $m^2.g^{-1}$ respectively. The higher surface area value of TNT is ascribed to one dimensional hollow structure having adsorption sites both exterior and interior of nanotubes. These results are in tune with our earlier reports [SOL MAT 2016].

Particle size and surface charge analysis

RSC Advances Accepted Manuscript

To understand the nature of surface charge and size of TFP or TNT, DLS and zeta potential analysis were carried out and results are displayed in Table 1. DLS data showed the particle size of TFP is 575 nm, which are about four folds higher than TEM analysis of the same particle, the higher size in suspension revealed the strong agglomeration behavior. On the other hand, TNT showed 295.3 nm, it is almost similar to TEM analysis, the size is explained through well dispersion in experimental medium. The zeta potential analysis of TFP and TNT showed -1.2 and -1.1 mV respectively.

Nano-TiO_2 decreased HMGB1 secretion from LPS induced RAW cells

HMGB1 is a ubiquitous nuclear protein, recently recognized as a pro-inflammatory mediator and an actively secreted cytokine by macrophages and apoptotic/necrotic cells upon cell injury and infection[8]. In this study we have investigated whether nano-TiO_2 inhibit the secretion of HMGB1 in LPS stimulated RAW 264.7 cells. As shown in the Fig. 3 enhanced HMGB1 secretion from LPS induced RAW 264.7 cells was observed and is co-related with previous studies[56,57]. Interestingly, cells treated with LPS and TNT or TFP at a concentration of 50µg/ml for 24h, we observed decreased HMGB1 secretion into culture supernatants (Fig.3). Recently, Neacsu *et al*. stated that TiO_2 nanotubes involved in the attenuation of inflammation *via* inhibition of mitogen-activated protein kinase (MAPK) nuclear factor kappa-light-chain-enhancer of activated B cells (NF-κB) pathways in RAW 264.7 cells[58]. Previous studies reported that HMGB1 activates the MAPK-NF-κB pathway by interacting with RAGE, and that it plays an important role in inflammation[59-61]. Probably, TNT and TFP reduce the HMGB1 levels by inhibiting the MAPK-NF-κB pathways.

Cytotoxicity of TNT and TFP on murine splenocytes

MLR is a model of T-cell response to alloantigenic peptide complex with major histocompatibility (MHC) proteins on antigen presenting complex (APC). Splenocytes from C57BL/6 mice were cultured in the presence of 10, 25, 50, 75, 100, 125 and 150µg/ml concentration of TNT and TFP for 24h. After 24h treatment, splenocytes of C57BL/6 mice (H-2^b) were inactivated with Mitomycin C and used as stimulators. In MLR, these stimulators were co-cultured with responder splenocytes of BALB/c mice (H-2^d) for 72h. TNT (Fig. 4A) and TFP (Fig. 4B) inhibited MLR in a dose dependent manner, with an IC_{50} value of 36.595µg/ml and

RSC Advances Accepted Manuscript

117.809μg/ml respectively for a 72 h co-culture. These results suggest that TNT and TFP probably block T cell mediated responses *in vitro*.

TNT and TFP ameliorates the EAE

C57BL/6 mice were used to determine the effect of TNT (protinic trititanate nanotubes) and TFP (TiO_2 fine particles) on evolution of EAE. Upon immunization with MOG_{35-55} peptide, mice developed clinical signs of EAE around day 8, reaching the peak of severity at about 18 days post induction. TNT or TFP (15mg/kg) administration on days 7 and 14 after EAE induction resulted a significant decrease in the severity of the disease according to the EAE score. TNT and TFP treated mice showed a mean clinical score 1.1 and 1.6 respectively at the peak of disease (day 18) compared with 3.5 clinical score of untreated mice as shown in Fig. 5A. Therefore compared with TFP treated mice, TNT treated mice effectively barred the EAE development.

TNT and TFP inhibits infiltration of inflammatory cells and degree of demyelination in the spinal cord

The effect of TNT and TFP treatment on central nervous system (CNS) infiltration was determined by H & E staining in the cross-section of the spinal cord. White matter of EAE mice spinal cord shows multiple foci of chronic inflammatory infiltrate with perivascular round cell collection and focal vacuolar degeneration. In contrast, TNT and TFP treated mice exhibited markedly decreased infiltration of inflammatory cells and focal vacuolar degeneration in the white matter of spinal cord (Fig. 7A).

To determine the degree of demyelination we stained sections of spinal cord with Luxol fast blue/ cresyl echt violet and observed wide spread demyelination zones in the white matter of spinal cord of EAE mice. In contrast, mice received TNT had minimal evidence of demyelination. Whereas occasional demyelination seen in grey matter of TFP treated spinal cord which is lesser than EAE group, is indicated by a markedly attenuated course of disease (Fig. 7B).

TNT and TFP inhibit *ex vivo* spleen cell proliferation

RSC Advances Accepted Manuscript

To investigate the mechanism in the regulation of EAE by TNT and TFP, we examined neural antigen-induced T cell proliferation in 24h, 48h and 72h culture. Splenocytes were isolated from each group of mice on day 23 and re-stimulated with MOG_{35-55} (20µg/ml) *in vitro*. When compared to EAE cells, spleen cells from EAE-TNT, EAE-TFP mice showed significant decrease in the T cells proliferation in response to *ex vivo* re-stimulation (Fig 5B). These results suggest that TNT and TFP ameliorate EAE by inhibiting the expansion of neural antigen specific T cells in C57BL/6 mice.

TNT and TFP suppress the HMGB1 cytokine production in EAE

HMGB1 released from activated immune cells or damaged, dying cells during necrosis and during the late phase of cellular apoptosis, is now recognized as a serum biomarker for EAE[20]. The expression and release of HMGB1 are significantly increased in various stages of EAE[62]. We aimed to test whether the administration of TNT/TFP on days 7 and 14 from the day of immunization suppress the HMGB1 production, as HMGB1 levels correlate with disease progression. C57BL/6 mice immunized with MOG_{35-55}/CFA were sacrificed at onset or peak of clinical disease and serum HMGB1 was quantified by ELISA. Compared to TNT/ TFP treated EAE mice, control untreated EAE mice had significantly elevated levels of HMGB1 in serum (Fig. 6A, $p < 0.05$). We further tested whether HMGB1 in peripheral blood correlated with *ex vivo* stimulation of splenocytes with MOG_{35-55} (20µg/ml). We observed higher concentrations of HMGB1in control untreated EAE splenocytes alone and in the presence of MOG_{35-55} (20µg/ml) when compared with TNT/ TFP treated EAE mice (Fig. 6B, $p < 0.05$). These results indicate that TNT/TFP inhibit the HMGB1secretion result in the reduction of disease pathogenesis.

Ameliorating function of TNT on arthritis model

We tested whether in addition to EAE model, TNT would also be effective for other autoimmune disease model. We used CIA model to evaluate the attenuation effect of TNT. Groups of 5 rats were immunized with collagen on days 0 and 7, subsequently on the same day of immunization injection of TNT (15mg/kg) *via* subcutaneously. Fig. 8A arthritis score shows untreated CIA group rats developed arthritis beginning from day 8 onwards and severe ankle swelling reaches on the day 18. However, TNT- treated group were significantly attenuated the incidence of

RSC Advances Accepted Manuscript

arthritis (~50%) and ankle swelling. The mean maximum arthritis score of CIA and CIA-TNT are 4 and 2 respectively.

The effect of TNT treatment on the histological changes in the ankle joints of rats and synovial tissue of the knee with CIA after the animals had been sacrificed on day 21 as shown in Fig. 9A and 9B. Histological evaluation showed that TNT inhibited synovial hyperplasia, inflammatory cell infiltration, cartilage erosion, and bone destruction, which were observed in CIA rats. Taken together, these results indicate that TNT administration results in a significant reduction of joint-tissue inflammation.

TNT inhibit the HMGB1 production in CIA

It has been demonstrated that HMGB-1 is the key proinflammatory cytokine that plays a crucial role in experimental arthritis models as well as in patients with arthritis[63,64]. Increased concentration of HMGB1 in CIA may serve as a biomarker for arthritis[65]. Serum was collected from 3 groups of rats on day 21. As shown in Fig. 8B, compared with control rat, rat with CIA showed increased circulating levels of HMGB1 in serum. In contrast CIA-TNT treated rat shows significantly reduced level of HMGB1.These results indicate that TNT treatment inhibit the HMGB1secretion result in the reduction of disease pathogenesis of CIA.

Discussion

EAE is the widely used animal model for MS. MS is driven by myelin-specific auto-reactive T cells that infiltrate the CNS and mediate an inflammatory response that result in demyelination and axon degradation[66]. EAE can be induced by immunization with a variety of myelin antigens. Among those MOG_{35-55} is an important candidate and MOG-reactive T cells also play significant roles in the pathogenesis of MS[67]. C57BL/6 mice develop chronic disease following immunization with MOG_{35-55} peptide.

In this study, we determined the role of TNT and TFP in the regulation of EAE model of MS. The administration of TNT and TFP on the day 7 and 14, appearance of clinical signs of EAE could control the evolution of the disease. To study the suppression of EAE by TNT and TFP, we analyzed the *in vitro* effect on the T cell recall response to MOG_{35-55} peptide. Treatment with TNT and TFP resulted in a significantly decreased proliferation by MOG_{35-55} *in vitro* experiments; this decreased proliferation was significantly stronger in TNT treated group.

RSC Advances Accepted Manuscript

HMGB1is a DNA-binding protein with proinflammatory properties, contributes to neuroinflammatory responses that drive EAE pathogenesis and that HMGB1 blockade may be a novel means to selectively disrupt the proinflammatory loop that drives MS autoimmunity. In the present study, extracellular HMGB1 was found to be increased in the sera and culture supernatant of *ex vivo* re-stimulation with MOG_{35-55} (20µg/ml) of EAE. HMGB1 levels co-relate with the disease severity of the EAE score, implicating a dynamic systemic inflammatory response. Previous studies have shown that, anti-HMGB1 antibody ameliorates EAE[21]. This is consistent with our HMGB1 cytokine levels in sera and *in vitro* re-stimulated culture. Histopathology results indicated that mice were rescued from EAE with less or no inflammatory cells as well as demyelination lesions in TNT and TFP treated EAE that are observed in EAE mice. TFP treated EAE found that relatively high inflammatory cells as well as demyelination lesions compared to TNT treated EAE.

We tested whether in addition to EAE model, TNT would also be effective for other autoimmune disease model. We demonstrated that the effect of TNT on CIA model, which has been the most widely used model of RA. This model has shortest duration between immunization and disease manifestation and shares several clinical, pathophysiological features with RA. Control SD rats were immunized with collagen on days 0 and 7and CIA-TNT rats immunized with collagen along with TNT (15mg/kg) on day 0 and 7. We observed that late onset with low severity of disease signs in CIA-TNT model compared with CIA model. Representative histological images of ankle joint tissue and knee synovial tissue showed that the administration of TNT into CIA model inhibit the cartilage degeneration, synovial hyperplasia with infiltration of inflammatory cells into the synovial tissue, which were observed in CIA model images. These results co-relate with the HMGB1 levels in the serum separated from CIA-TNT group rat blood. HMGB1 is a novel proinflammatory cytokine, involved in the pathogenesis of RA. Extracellular HMGB1 induces the secretion of proinflammatory cytokine TNF, IL-1, and IL-6 from macrophages/damaged cells[12]. Taniguchi *et al*. reported that high level of HMGB1 expression in the synovium of RA patients as well as adjuvant-induced arthritis and CIA[63]. Administration of HMGB1 into mice joints, itself induce joint inflammation by activating monocytes/ macrophages and inducing proinflammatory cytokines leads to arthritis changes [68]. Experimental arthritis could be effectively treated by the administration of polyclonal and monoclonal anti-HMGB1antibodies which are specific for the HMGB1 cytokine[22 69]. HMGB1 play a key role in

RSC Advances Accepted Manuscript

the development and disease progression of the arthritis. Interestingly, our results indicated that CIA serum shows high levels of HMGB1cytokine compared with TNT treated group of rats. With this we found that TNT effectively reduced the clinical signs and pathophysiology of arthritis in CIA-TNT model. To the best of our knowledge, this is the first study to show that administration of TNT/TFP can reduce the EAE and CIA pathogenesis.

In conclusion, our findings suggest that Ti-O based nanomaterials administration ameliorated the clinical severity of EAE (TNT/TFP), CIA (TNT) significantly by ameliorating pathology, and presumably attenuating the immune response *via* HMGB1 cytokine release. Finally we suggest that, TNT and TFP may have therapeutic potential not only for MS, RA but also for other autoimmune disorders.

Acknowledgements

This work was supported by grants from Science and Engineering Research Board (SERB), India (Grant #: SR/FT/LS-149/2010) and Council of scientific and industrial research (CSIR), India, (Grant# 37(1517)/11/EMR-II) to Dakshayani Lomada and University Grants Commission, New Delhi (UGC F. No: 42-176/2013(SR)) to Madhava C Reddy

References

1. A. Compston and A. Coles, *Lancet*, 2008, **372**, 1502-1517.
2. V. Browning, M. Joseph and M. Sedrak, *JAAPA : official journal of the American Academy of Physician Assistants*, 2012, **25**, 24-29.
3. T. M. Rivers, D. H. Sprunt and G. P. Berry, *J Exp Med*, 1933, **58**, 39-53.
4. I. Mendel, N. Kerlero de Rosbo and A. Ben-Nun, *European journal of immunology*, 1995, **25**, 1951-1959.
5. B. Joe and R. L. Wilder, *Molecular medicine today*, 1999, **5**, 367-369.
6. P. Brooks and P. Kubler, *Therapeutics and clinical risk management*, 2006, **2**, 45-57.
7. P. E. Lipsky, L. S. Davis, J. J. Cush and N. Oppenheimer-Marks, *Springer seminars in immunopathology*, 1989, **11**, 123-162.
8. R. Kang, R. Chen, Q. Zhang, W. Hou, S. Wu, L. Cao, J. Huang, Y. Yu, X. G. Fan, Z. Yan, X. Sun, H. Wang, Q. Wang, A. Tsung, T. R. Billiar, H. J. Zeh, 3rd, M. T. Lotze and D. Tang, *Molecular aspects of medicine*, 2014, **40**, 1-116.
9. M. C. Reddy and K. M. Vasquez, *Radiation research*, 2005, **164**, 345-356.
10. P. Scaffidi, T. Misteli and M. E. Bianchi, *Nature*, 2002, **418**, 191-195.
11. J. Tian, A. M. Avalos, S. Y. Mao, B. Chen, K. Senthil, H. Wu, P. Parroche, S. Drabic, D. Golenbock, C. Sirois, J. Hua, L. L. An, L. Audoly, G. La Rosa, A. Bierhaus, P. Naworth, A. Marshak-Rothstein, M. K. Crow, K. A. Fitzgerald, E. Latz, P. A. Kiener and A. J. Coyle, *Nature immunology*, 2007, **8**, 487-496.

RSC Advances Accepted Manuscript

12. U. Andersson, H. Wang, K. Palmblad, A. C. Aveberger, O. Bloom, H. Erlandsson-Harris, A. Janson, R. Kokkola, M. Zhang, H. Yang and K. J. Tracey, *The Journal of experimental medicine*, 2000, **192**, 565-570.
13. A. Rouhiainen, J. Kuja-Panula, E. Wilkman, J. Pakkanen, J. Stenfors, R. K. Tuominen, M. Lepantalo, O. Carpen, J. Parkkinen and H. Rauvala, *Blood*, 2004, **104**, 1174-1182.
14. M. Magna and D. S. Pisetsky, *Molecular medicine (Cambridge, Mass.)*, 2014, **20**, 138-146.
15. E. Sundberg, A. E. Fasth, K. Palmblad, H. E. Harris and U. Andersson, *Immunobiology*, 2009, **214**, 303-309.
16. J. M. Reynolds, G. J. Martinez, Y. Chung and C. Dong, *Proc Natl Acad Sci U S A*, 2012, **109**, 13064-13069.
17. I. Stojanovic, S. Cuzzocrea, K. Mangano, E. Mazzon, D. Miljkovic, M. Wang, M. Donia, Y. Al Abed, J. Kim, F. Nicoletti, S. Stosic-Grujicic and M. Claesson, *Clin Immunol*, 2007, **123**, 311-323.
18. A. Andersson, R. Covacu, D. Sunnemark, A. I. Danilov, A. Dal Bianco, M. Khademi, E. Wallstrom, A. Lobell, L. Brundin, H. Lassmann and R. A. Harris, *Journal of leukocyte biology*, 2008, **84**, 1248-1255.
19. R. S. Goldstein, A. Bruchfeld, L. Yang, A. R. Qureshi, M. Gallowitsch-Puerta, N. B. Patel, B. J. Huston, S. Chavan, M. Rosas-Ballina, P. K. Gregersen, C. J. Czura, R. P. Sloan, A. E. Sama and K. J. Tracey, *Molecular medicine (Cambridge, Mass.)*, 2007, **13**, 210-215.
20. A. P. Robinson, M. W. Caldis, C. T. Harp, G. E. Goings and S. D. Miller, *Journal of autoimmunity*, 2013, **43**, 32-43.
21. A. Uzawa, M. Mori, J. Taniguchi, S. Masuda, M. Muto and S. Kuwabara, *Clinical and experimental immunology*, 2013, **172**, 37-43.
22. R. Kokkola, J. Li, E. Sundberg, A. C. Aveberger, K. Palmblad, H. Yang, K. J. Tracey, U. Andersson and H. E. Harris, *Arthritis and rheumatism*, 2003, **48**, 2052-2058.
23. S. Malhotra, N. Fissolo, M. Tintore, A. C. Wing, J. Castillo, A. Vidal-Jordana, X. Montalban and M. Comabella, *Journal of neuroinflammation*, 2015, **12**, 48.
24. J. M. Escandell, M. C. Recio, S. Manez, R. M. Giner, M. Cerda-Nicolas and J. L. Rios, *The Journal of pharmacology and experimental therapeutics*, 2007, **320**, 581-590.
25. T. Minko, L. Rodriguez-Rodriguez and V. Pozharov, *Advanced drug delivery reviews*, 2013, **65**, 1880-1895.
26. Y. Diebold, M. Jarrin, V. Saez, E. L. Carvalho, M. Orea, M. Calonge, B. Seijo and M. J. Alonso, *Biomaterials*, 2007, **28**, 1553-1564.
27. P. Debbage, *Current pharmaceutical design*, 2009, **15**, 153-172.
28. R. A. Maldonado, R. A. LaMothe, J. D. Ferrari, A. H. Zhang, R. J. Rossi, P. N. Kolte, A. P. Griset, C. O'Neil, D. H. Altreuter, E. Browning, L. Johnston, O. C. Farokhzad, R. Langer, D. W. Scott, U. H. von Andrian and T. K. Kishimoto, *Proceedings of the National Academy of Sciences of the United States of America*, 2015, **112**, E156-165.
29. A. Yeste, M. Nadeau, E. J. Burns, H. L. Weiner and F. J. Quintana, *Proceedings of the National Academy of Sciences of the United States of America*, 2012, **109**, 11270-11275.
30. M. Donia, K. Mangano, C. Quattrocchi, P. Fagone, S. Signorelli, G. Magro, A. Sfacteria, K. Bendtzen and F. Nicoletti, *Scand J Immunol*, 2010, **72**, 396-407.
31. T. Takagi, P. W. Tsao, R. Totsuka, T. Suzuki, T. Murata and I. Takata, *Jpn J Pharmacol*, 1998, **78**, 225-228.

RSC Advances Accepted Manuscript

32. H. W. Minne, J. Pfeilschifter, S. Scharla, S. Mutschelknauss, A. Schwarz, B. Krempien and R. Ziegler, *Endocrinology*, 1984, **115**, 50-54.
33. K. Mangano, A. Nicoletti, F. Patti, M. Donia, L. Malaguarnera, S. Signorelli, G. Magro, V. Muzio, B. Greco, P. Zaratin, P. Meroni, M. Zappia and F. Nicoletti, *Clin Exp Immunol*, 2010, **159**, 159-168.
34. J. H. Duarte, *Nature reviews. Rheumatology*, 2015, **11**, 319.
35. A. L. Dellinger, P. Cunin, D. Lee, A. L. Kung, D. B. Brooks, Z. Zhou, P. A. Nigrovic and C. L. Kepley, *PloS one*, 2015, **10**, e0126290.
36. K. Yudoh, R. Karasawa, K. Masuko and T. Kato, *International journal of nanomedicine*, 2009, **4**, 217-225.
37. C. Y. Tsai, A. L. Shiau, S. Y. Chen, Y. H. Chen, P. C. Cheng, M. Y. Chang, D. H. Chen, C. H. Chou, C. R. Wang and C. L. Wu, *Arthritis and rheumatism*, 2007, **56**, 544-554.
38. L. Leonaviciene, G. Kirdaite, R. Bradunaite, D. Vaitkiene, A. Vasiliauskas, D. Zabulyte, A. Ramanaviciene, A. Ramanavicius, T. Asmenavicius and Z. Mackiewicz, *Medicina (Kaunas, Lithuania)*, 2012, **48**, 91-101.
39. N. Nagai and Y. Ito, *Biological & pharmaceutical bulletin*, 2014, **37**, 96-104.
40. W. U. Kim, W. K. Lee, J. W. Ryoo, S. H. Kim, J. Kim, J. Youn, S. Y. Min, E. Y. Bae, S. Y. Hwang, S. H. Park, C. S. Cho, J. S. Park and H. Y. Kim, *Arthritis and rheumatism*, 2002, **46**, 1109-1120.
41. S. M. Moghimi, A. C. Hunter and J. C. Murray, *FASEB journal : official publication of the Federation of American Societies for Experimental Biology*, 2005, **19**, 311-330.
42. N. Sanvicens and M. P. Marco, *Trends in biotechnology*, 2008, **26**, 425-433.
43. W. W. Brien, E. A. Salvati, F. Betts, P. Bullough, T. Wright, C. Rimnac, R. Buly and K. Garvin, *Clinical orthopaedics and related research*, 1992, 66-74.
44. R. S. Flatebo, A. C. Johannessen, A. G. Gronningsaeter, O. E. Boe, N. R. Gjerdet, B. Grung and K. N. Leknes, *Journal of periodontology*, 2006, **77**, 1201-1210.
45. H. Schliephake, H. Lehmann, U. Kunz and R. Schmelzeisen, *International journal of oral and maxillofacial surgery*, 1993, **22**, 20-25.
46. Y. Chen, Y. Wan, Y. Wang, H. Zhang and Z. Jiao, *International journal of nanomedicine*, 2011, **6**, 2321-2326.
47. J. Xu, Y. Sun, J. Huang, C. Chen, G. Liu, Y. Jiang, Y. Zhao and Z. Jiang, *Bioelectrochemistry (Amsterdam, Netherlands)*, 2007, **71**, 217-222.
48. B. C. Schanen, A. S. Karakoti, S. Seal, D. R. Drake, 3rd, W. L. Warren and W. T. Self, *ACS nano*, 2009, **3**, 2523-2532.
49. R. K. Shukla, A. Kumar, D. Gurbani, A. K. Pandey, S. Singh and A. Dhawan, *Nanotoxicology*, 2013, **7**, 48-60.
50. J. Xu, H. Shi, M. Ruth, H. Yu, L. Lazar, B. Zou, C. Yang, A. Wu and J. Zhao, *PloS one*, 2013, **8**, e70618.
51. H. Shi, R. Magaye, V. Castranova and J. Zhao, *Particle and fibre toxicology*, 2013, **10**, 15.
52. G. Oberdorster, J. Ferin and B. E. Lehnert, *Environmental health perspectives*, 1994, **102 Suppl 5**, 173-179.
53. D. Praveen Kumar, M. V. Shankar, M. M. Kumari, G. Sadanandam, B. Srinivas and V. Durgakumari, *Chemical communications (Cambridge, England)*, 2013, **49**, 9443-9445.
54. T. Itoh, K. Ishii, T. Irikura, Y. Ueno, A. Kojima and Y. Horie, *J Antibiot (Tokyo)*, 1993, **46**, 1575-1581.

RSC Advances Accepted Manuscript

55. V. Krenn, L. Morawietz, G. R. Burmester, R. W. Kinne, U. Mueller-Ladner, B. Muller and T. Haupl, *Histopathology*, 2006, **49**, 358-364.
56. D. Tang, Y. Shi, R. Kang, T. Li, W. Xiao, H. Wang and X. Xiao, *Journal of leukocyte biology*, 2007, **81**, 741-747.
57. S. Cao, S. Li, H. Li, L. Xiong, Y. Zhou, J. Fan, X. Yu and H. Mao, *PloS one*, 2013, **8**, e54647.
58. P. Neacsu, A. Mazare, P. Schmuki and A. Cimpean, *Int J Nanomedicine*, 2015, **10**, 6455-6467.
59. J. A. Nogueira-Machado, C. M. Volpe, C. A. Veloso and M. M. Chaves, *Expert Opin Ther Targets*, 2011, **15**, 1023-1035.
60. U. Andersson and H. Rauvala, *J Intern Med*, 2011, **270**, 296-300.
61. R. Vitali, L. Stronati, A. Negroni, G. Di Nardo, M. Pierdomenico, E. del Giudice, P. Rossi and S. Cucchiara, *Am J Gastroenterol*, 2011, **106**, 2029-2040.
62. Y. Sun, H. Chen, J. Dai, H. Zou, M. Gao, H. Wu, B. Ming, L. Lai, Y. Xiao, P. Xiong, Y. Xu, F. Gong and F. Zheng, *Journal of neuroimmunology*, 2015, **280**, 29-35.
63. N. Taniguchi, K. Kawahara, K. Yone, T. Hashiguchi, M. Yamakuchi, M. Goto, K. Inoue, S. Yamada, K. Ijiri, S. Matsunaga, T. Nakajima, S. Komiya and I. Maruyama, *Arthritis and rheumatism*, 2003, **48**, 971-981.
64. R. Kokkola, E. Sundberg, A. K. Ulfgren, K. Palmblad, J. Li, H. Wang, L. Ulloa, H. Yang, X. J. Yan, R. Furie, N. Chiorazzi, K. J. Tracey, U. Andersson and H. E. Harris, *Arthritis and rheumatism*, 2002, **46**, 2598-2603.
65. U. Andersson and H. E. Harris, *Biochimica et biophysica acta*, 2010, **1799**, 141-148.
66. C. S. Constantinescu, N. Farooqi, K. O'Brien and B. Gran, *British journal of pharmacology*, 2011, **164**, 1079-1106.
67. H. Shao, Z. Huang, S. L. Sun, H. J. Kaplan and D. Sun, *Investigative ophthalmology & visual science*, 2004, **45**, 4060-4065.
68. R. Pullerits, I. M. Jonsson, M. Verdrengh, M. Bokarewa, U. Andersson, H. Erlandsson-Harris and A. Tarkowski, *Arthritis and rheumatism*, 2003, **48**, 1693-1700.
69. H. Schierbeck, P. Lundback, K. Palmblad, L. Klevenvall, H. Erlandsson-Harris, U. Andersson and L. Ottosson, *Molecular medicine (Cambridge, Mass.)*, 2011, **17**, 1039-1044.

RSC Advances Accepted Manuscript

Figure legends

Fig. 1. TEM image of TFP and TNT nanomaterials

Fig. 2. XRD pattern of TFP and TNT nanomaterials

Fig. 3. Nanomaterials TNT and TFP decreased the release of HMGB1 in LPS-induced RAW cells. RAW 264.7 cells were treated with LPS in the presence or absence of TNT or TFP at a concentration of 50μg/ml for 24h. After incubation, culture supernatant were collected and subjected to ELISA for quantification of HMGB1. Data are presented as mean ± SD of three independent experiments. Statistical significance was defined as *$p < 0.05$.

Fig. 4. Cytotoxicity of TNT and TFP in mixed lymphocyte reaction (MLR) of mice splenocytes using the MTT assay on a 72h culture. TNT (Fig. 4A) and TFP (Fig. 4B) inhibited MLR in a dose dependent manner, with an IC_{50} value of 36.5μg/ml and 117.8μg/ml respectively for a 72 h co-culture.

Fig. 5. EAE-TNT, EAE-TFP mice developed an attenuated and delayed course of EAE. C57BL/6 mice were induced to develop EAE by immunization with MOG_{35-55} peptide and treated one group with 15mg/kg of TNT and other group with TFP on the days 7 and 14 via intraperitonially (A).The clinical scores were evaluated daily and were plotted as the mean ± SD (n=5/group). Maximum clinical scores as well as scores on day 18 and 22 evidence marked attenuation of disease severity after TNT and TFP administration. (B). Spleen cells were isolated on day 23 from each group and stimulated with MOG_{35-55} antigen (20μg/ml) *ex vivo* for 24h, 48h and 72h. Proliferation response was measured by MTT assay. The data are presented as mean ± SD (*$p<0.05$).

Fig. 6. TNT and TFP suppress the HMGB1 cytokine production in EAE. (A).The immunized mice were euthanized on day 23, the serum was collected from each group of mice and amount of HMGB1was analyzed by ELISA. The concentration of HMGB1 was calculated using the standard plot and shown as mean ± SD ($p<0.05$). (B). Spleen cells were cultured with MOG_{35-55} peptide (20μg/ml) *ex vivo* for 48h, culture supernatants were collected and concentration of HMGB1 was determined by ELISA. The data are presented as mean ± SD (*$p<0.05$).

Fig. 7. Attenuation of inflammation progression and demyelination in the CNS region of mice that received EAE-TNT and EAE-TFP, spinal cords from each group of mice were removed on day 23. In EAE-TNT mice, the number of immune-cell infiltrates (H & E, Fig 7A-c) and demyelination (Luxol fast blue, Fig 7B-c) were both significantly reduced. (A) Hematoxylin and Eosin staining. (B) Luxol fast blue staining. a. Control, b. EAE, c. EAE-TNT, d. EAE-TFP.

Fig. 8. Amelioration functions of TNT on CIA model. Rats were immunized with collagen on days 0 and 7, followed by administration of TNT (15mg/kg) subcutaneously on day 0 and 7. Arthritis score, the levels of arthritis measurements were taken every two days (A). At the day 21 all rats were sacrificed and blood was collected by cardiac puncture, serum was separated and quantified the HMGB1 cytokine (B). TNT inhibit the proinflammatory HMGB1 levels in CIA-TNT model and protects from the inflammatory arthritis. The data are presented as mean ± SD ($^{*}p<0.05$).

RSC Advances Accepted Manuscript

Fig. 9. Representative hematoxylin and eosin micrographs of joint tissue in arthritis model compared with TNT treated rats with CIA. Ankle joint tissue (A), synovium tissue of knee (B), showed synovial hyperplasia and infiltration of inflammatory cells in untreated CIA and relatively less or no inflammatory cells, damage to the synovial membrane of TNT-CIA.

Table.1. Zeta potential evaluation and DLS analysis for TFP and TNT

RSC Advances Accepted Manuscript

Figure 1:

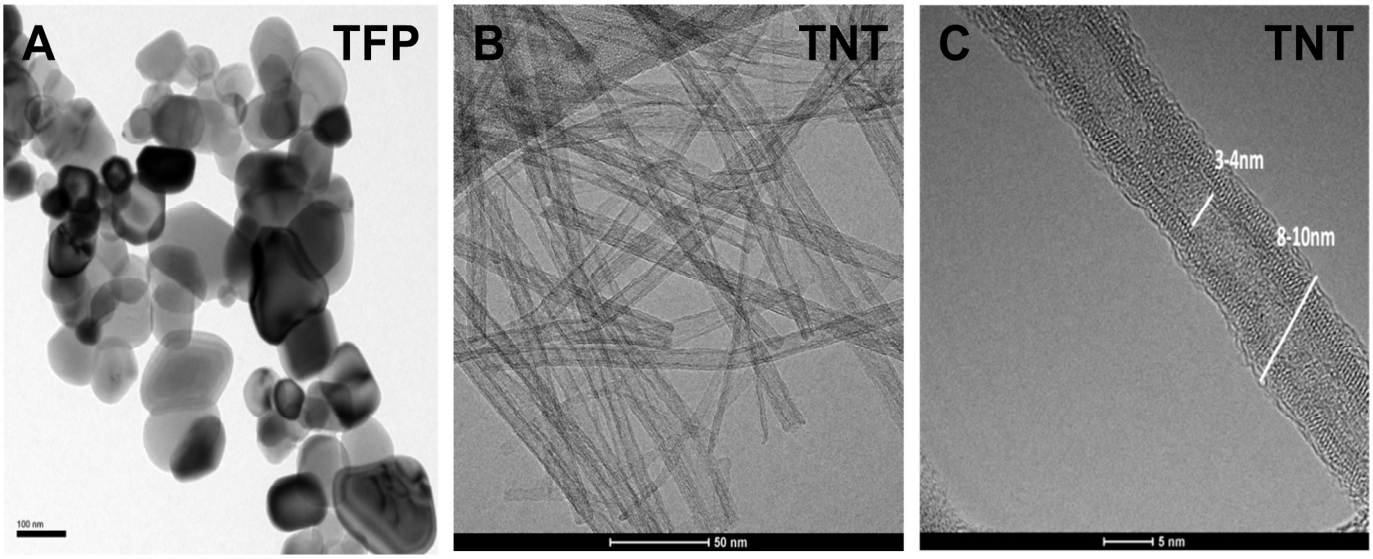

RSC Advances Accepted Manuscript

Figure 2:

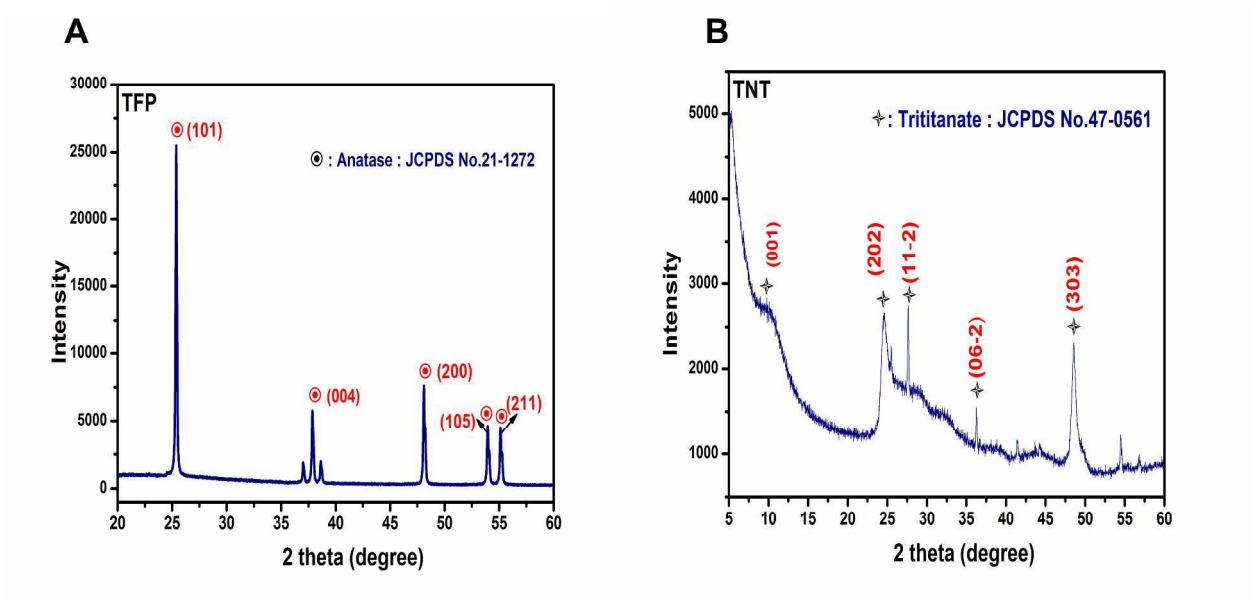

RSC Advances Accepted Manuscript

Figure 3:

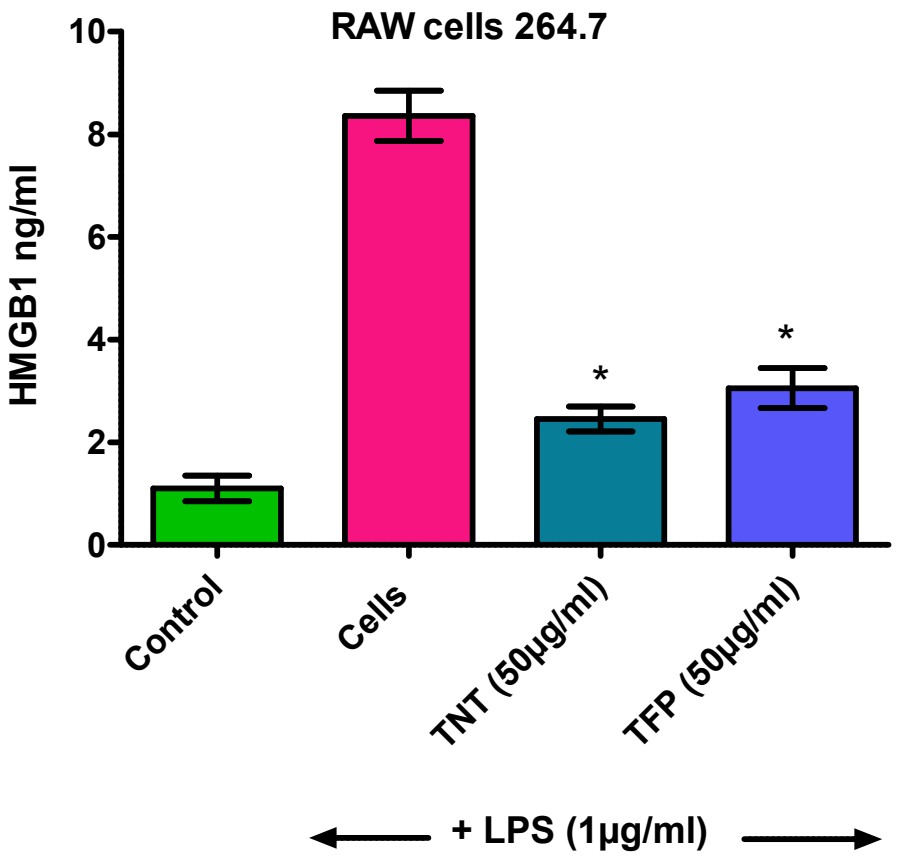

RSC Advances Accepted Manuscript

Figure 4:

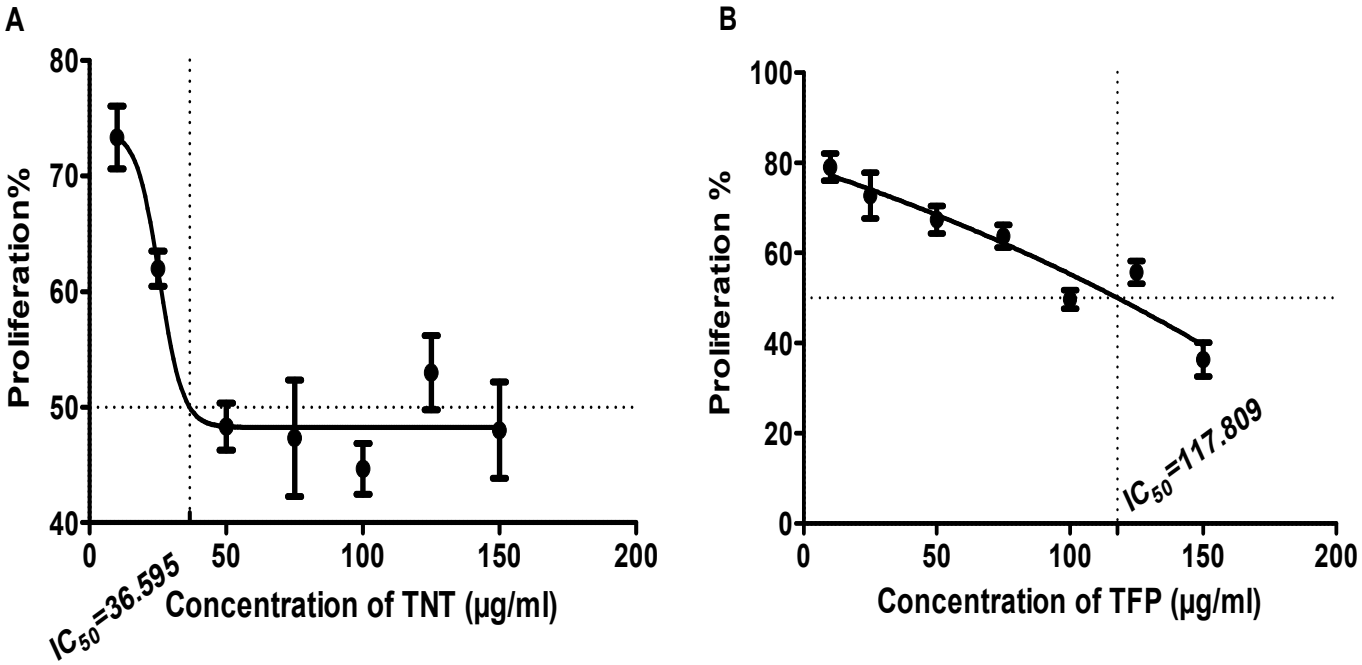

RSC Advances Accepted Manuscript

Figure 5:

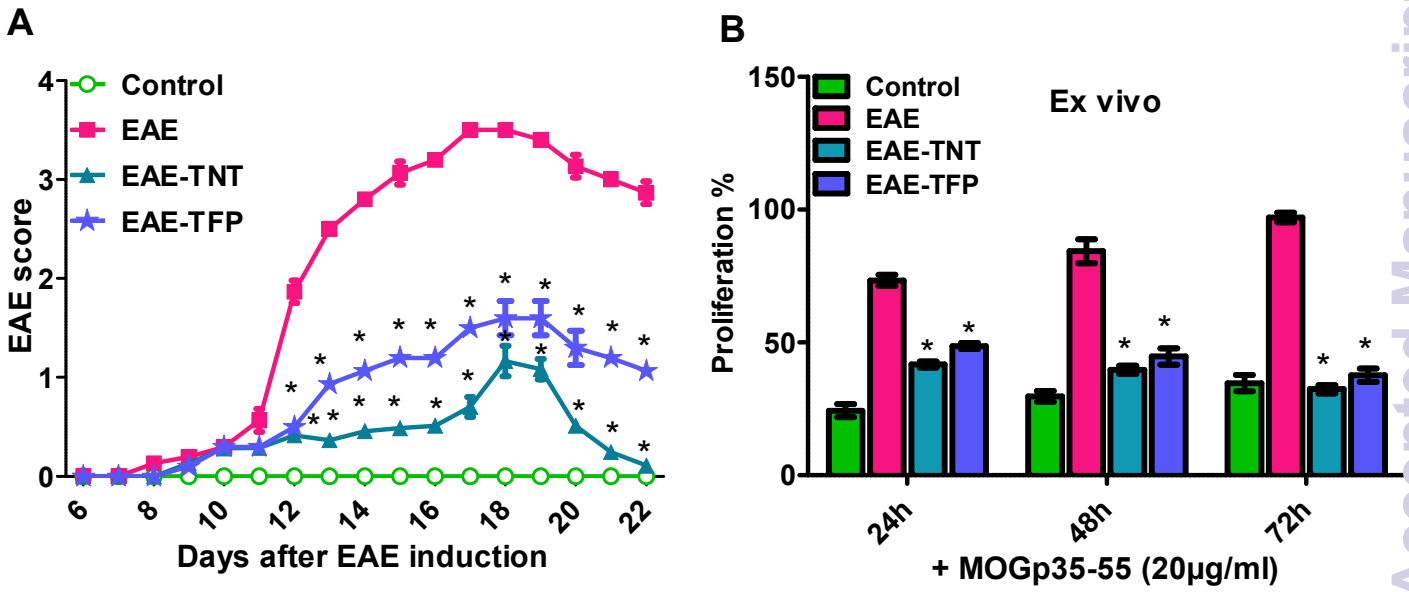

RSC Advances Accepted Manuscript

Figure 6:

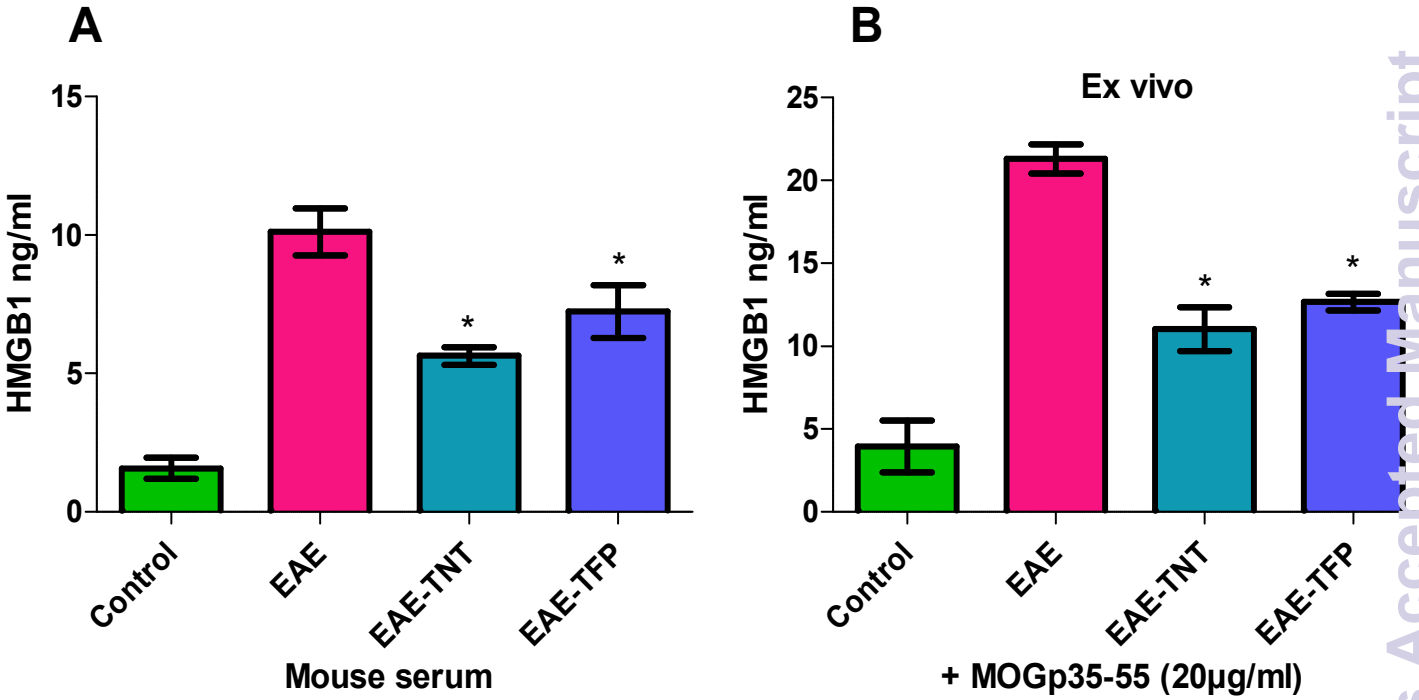

RSC Advances Accepted Manuscript

Figure 7:

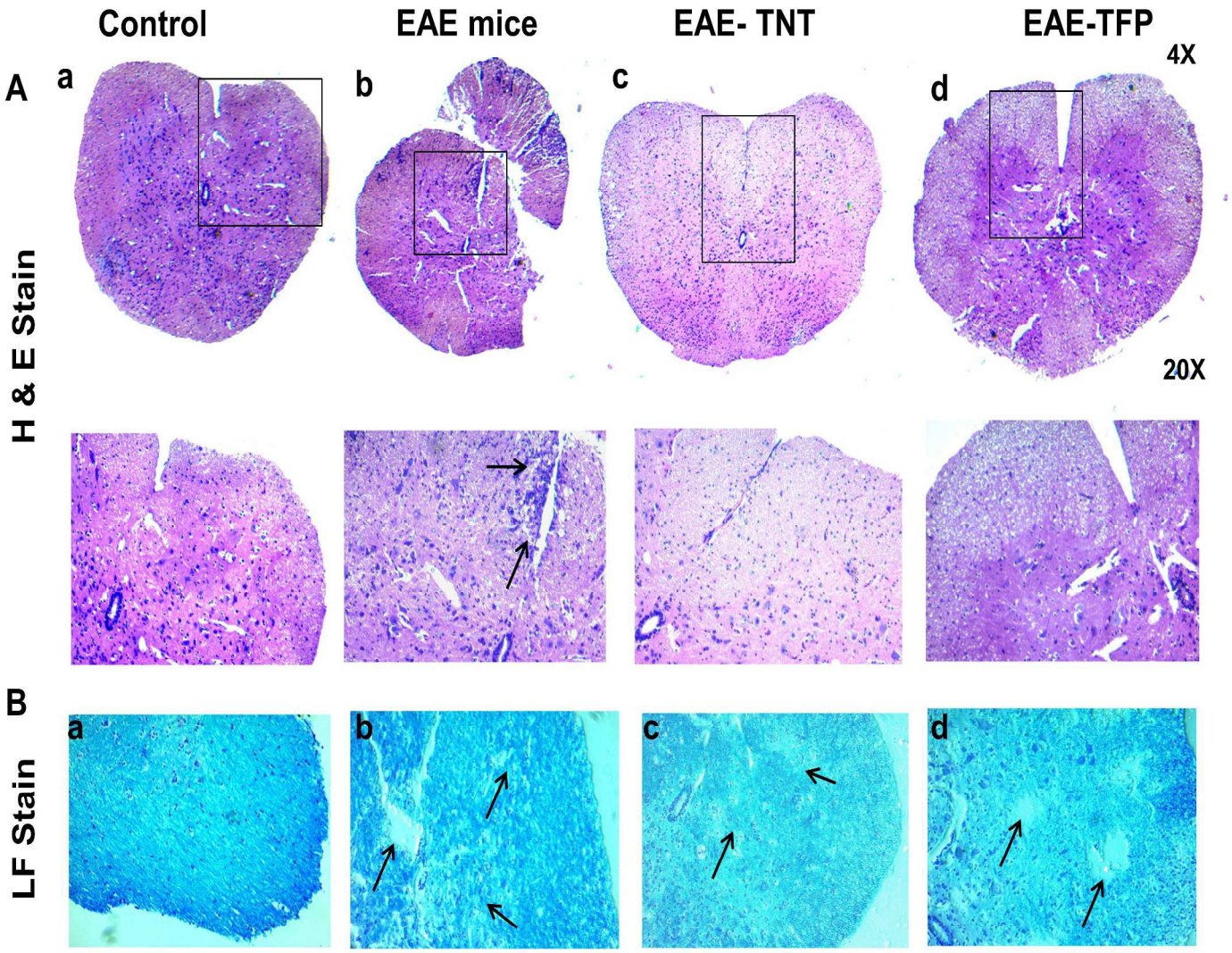

RSC Advances Accepted Manuscript

Figure 8:

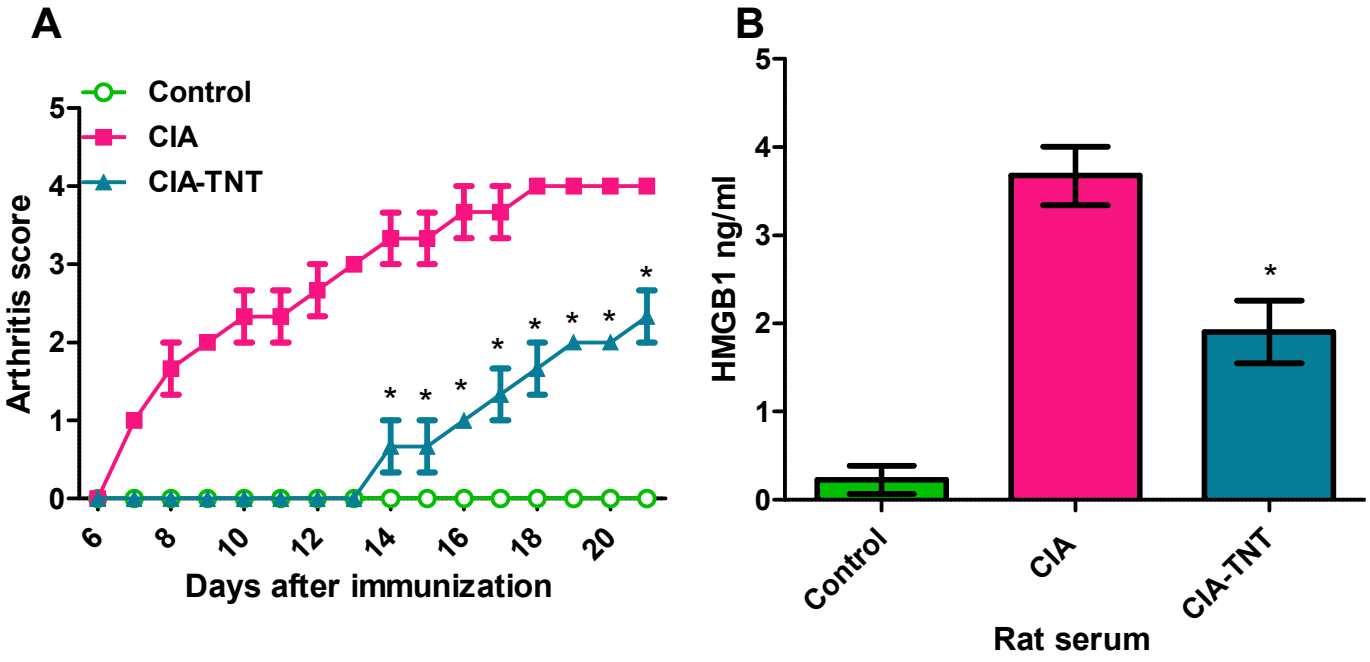

RSC Advances Accepted Manuscript

Figure 9:

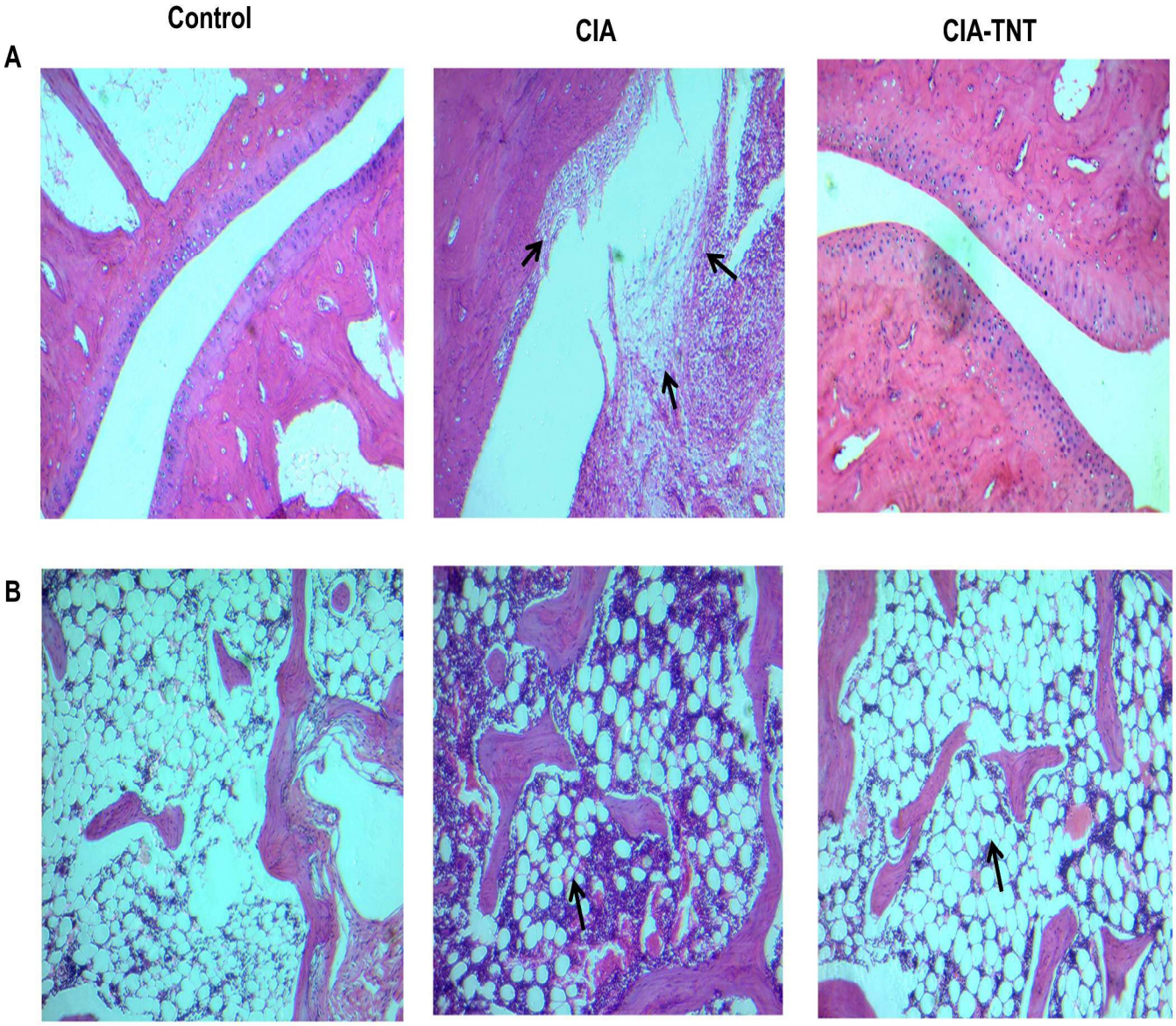

RSC Advances Accepted Manuscript

Table 1.

Sl.No.	Sample ID	Particle size analysis (nm)	Zeta Potential (mV)
1.	TFP	575	-1.2
2.	TNT	295.3	-1.1

RSC Advances Accepted Manuscript